Spherical Wave Scattering Matrix Description of Antenna Coupling in Arbitrary Environments

Ryan J. Pirkl, *Member, IEEE*

***Abstract*—A framework is presented for investigating antenna coupling in arbitrary environments by way of antenna and environment scattering parameter matrices. The environment scattering parameter matrices are *bona fide* scattering parameters that describe the environment when all radiation ports are terminated with nonreflecting loads. Simplification of the antenna coupling equations leads to a second formulation that is compatible with classically-defined antenna scattering parameter matrices. A third formulation, based on an auxiliary set of matrices describing the environment's scattering when all unexcited radiation ports are open-circuited, extends the coupling formulation used in spherical near-field antenna measurements to arbitrary environments.**

***Index Terms*—Antenna coupling, antenna scattering parameters, environment impedance parameters, environment scattering parameters, spherical modal signal flow graph, spherical waves.**

I. Introduction

COUPLING between antennas in arbitrary environments is expressed in terms of spherical modal scattering parameter matrices for the antenna and the environment. This enables a complete mathematical description of both antenna-antenna and antenna-environment interactions. This work was motivated by a need to characterize such interactions in severe scattering environments such as a reverberation chamber.

Antenna–antenna coupling in anechoic (i.e., nominally free-space) environments forms the mathematical theory underlying near-field antenna measurements [1]–[8]. Equations describing how two antennas interact with respect to some bounding planar [2], cylindrical [3], or spherical [6] surface have enabled the development of near-field antenna characterization techniques based on scattering parameter measurements obtained on these bounding surfaces. Extensions of the spherical near-field antenna coupling equations have been used to characterize bistatic scattering from objects [9], mutual coupling between antenna array elements [10], and channel matrices for multiple-input multiple-output antenna systems in free-space [11].

More complicated scattering environments have been analyzed by describing the scattering between multiple objects in terms of each object's T-matrix [12], [13]. The T-matrix describes the spherical modal scattering characteristics of a pure scatterer and is applicable to environments featuring localized scatterers in free-space. In a series of papers, Felsen *et al.* presented a domain decomposition framework for analyzing arbitrary scattering environments where the solution to the overall scattering problem was formulated in terms of coupling between subdomain solutions [14]–[16]. In [17], a variation of this domain decomposition technique was used to describe coupling between isolated subdomains in terms of radially propagating beams. In [18] and [19], a domain decomposition approach based on a spherical interface surrounding an antenna was used to evaluate the change in an antenna's input impedance due to a nearby scatterer.

Here, we employ a variation of the domain decomposition techniques described in [14] and [17]–[19] that allows us to treat the environment's scatterers in aggregate through environment-specific modal excitation functions. These functions provide a compact description of the environment's response to a spherical modal excitation that enables the free-space spherical antenna coupling equations to be generalized to arbitrary environments. We present the complete coupling formulation in Section II along with qualitative descriptions of the antenna and environment scattering parameters. Then, in Section III, we define the environment's scattering parameter matrices in terms of its impedance parameter matrices and relate these impedance parameter matrices to the environment's total field response to a spherical modal current source. Two alternative coupling formulations are presented in Section IV. In Section V, the formulations are validated by way of simulations of coupling between a pair of infinitesimal dipole antennas in both free-space and a rectangular cavity. Applications and possible extensions of this work are discussed in Section VI. A summary is given in Section VII.

II. Coupling Formulation

Fig. 1 describes antenna-antenna and antenna-environment interactions in an arbitrary environment by use of a signal flow graph. The spherical modal signal flow graph describes the characteristics of the environment and each antenna in terms of scattering parameters relating inward and outward going waves at different "ports." The "ports" in Fig. 1 are the physical antenna ports as well as radiation ports at the spherical interfaces, Ω_1 and Ω_2, bounding each of the antennas. Fig. 1(a) presents a partial signal flow graph description that also illustrates the physical aspects of the problem; the full signal flow graph is presented in Fig. 1(b). Simplifications of Fig. 1(b) have been previously used to describe antenna-antenna interactions for spherical near-field antenna measurements in anechoic (i.e., nominally free-space) environments [6] as well as for a single antenna in the presence of a scatterer [18], [19].

Manuscript received December 12, 2011; revised April 20, 2012; accepted June 26, 2012. Date of publication August 06, 2012; date of current version November 29, 2012. This work was supported by a National Research Council Postdoctoral Research Associateship.

The author is with the RF Fields Group, Electromagnetics Division, National Institute of Standards and Technology, Boulder, CO 80305 USA (e-mail: rpirkl@gmail.com).

Color versions of one or more of the figures in this paper are available online at http://ieeexplore.ieee.org.

Digital Object Identifier 10.1109/TAP.2012.2211851

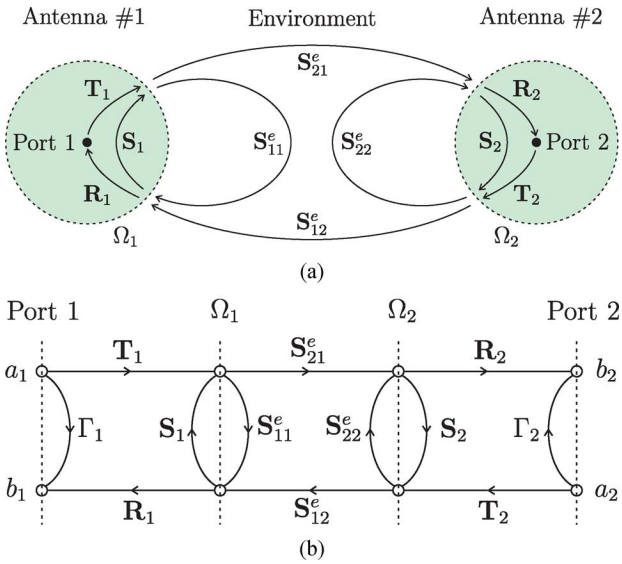

Fig. 1. Description of coupling between antennas in an arbitrary environment. (a) Diagram representation. (b) Signal flow graph representation.

We specify that the antenna and environment scattering parameters are defined with respect to the characteristic impedances of the radiation and antenna ports. For convenience, we impose the constraint that the characteristic impedances of the antennas' physical ports be identical. We also emphasize that the antenna and environment scattering parameters described in Fig. 1 are defined with respect to spherical interfaces, Ω_1 and Ω_2, of *finite* radii. This is in contrast to the classically-defined antenna scattering parameters (e.g., those presented in [6]) that are defined with respect to spherical interfaces of *infinite* radius. We revisit this point in Section IV, where we present an alternative formulation that is compatible with the classically-defined antenna scattering parameters.

The following sections present a qualitative description of the antenna and environment scattering parameter matrices used in Fig. 1's signal flow graph and the associated coupling equations for two antennas in an arbitrary environment. A rigorous mathematical definition of the environment scattering parameter matrices is given later in Section III.

A. Antenna Scattering Parameter Matrices

An antenna may be described by four scattering parameters analogous to the scattering parameters of a typical two-port system [6]. With respect to antenna #1, $\Gamma_1 \in \mathbb{C}^{1\times 1}$ is a complex scalar describing the antenna's free-space reflection coefficient, $\mathbf{T}_1 \in \mathbb{C}^{P_1\times 1}$ is a complex column vector describing the antenna's transmit properties, $\mathbf{R}_1 \in \mathbb{C}^{1\times P_1}$ is a complex row vector describing the antenna's receive properties, and $\mathbf{S}_1 \in \mathbb{C}^{P_1\times P_1}$ is a complex matrix describing the antenna's bistatic scattering properties. The reflection coefficient Γ_1 is defined at "Port 1" in Fig. 1; the transmission, reception, and scattering properties are defined at radiation ports located on the spherical interface Ω_1 bounding the antenna. The quantity P_1 is the finite number of spherical modes required to describe the antenna's transmitting, receiving, and scattering characteristics [6], [20]. The description of antenna #2 is analogous with Γ_2 defined at "Port 2," and $\mathbf{T}_2 \in \mathbb{C}^{P_2\times 1}$, $\mathbf{R}_2 \in \mathbb{C}^{1\times P_2}$, and $\mathbf{S}_2 \in \mathbb{C}^{P_2\times P_2}$ defined at radiation ports located on the bounding spherical interface Ω_2. Following the classical scattering matrix description of antenna coupling, we define the bistatic scattering matrix of free space as an identity matrix, $\mathbf{I}$, whereby the bistatic scattering matrix $\mathbf{S}_{1,2}$ describes the total (i.e., incident plus scattered) field arising when a set of inward propagating waves impinge on the antenna [6].

B. Environment Scattering Parameter Matrices

The environment may likewise be described by four scattering parameters: $\mathbf{S}^e_{11} \in \mathbb{C}^{P_1\times P_1}$, $\mathbf{S}^e_{21} \in \mathbb{C}^{P_2\times P_1}$, $\mathbf{S}^e_{22} \in \mathbb{C}^{P_2\times P_2}$, and $\mathbf{S}^e_{12} \in \mathbb{C}^{P_1\times P_2}$. The matrix $\mathbf{S}^e_{uv}$ with $u = 1, 2$ and $v = 1, 2$ relates the P_v outward propagating spherical waves at Ω_u to the P_v inward propagating spherical waves at Ω_u. We emphasize that, like the antenna scattering parameters, $\mathbf{S}^e_{uv}$ are *bona fide* scattering parameters defined when all radiation ports are terminated with perfectly matched loads.

C. Coupling Equations for Two Antennas in an Arbitrary Environment

Starting from the signal flow graph presented in Fig. 1(b), conventional signal flow graph manipulations[1] or, alternatively, matrix manipulations may be used to solve for the four scalar scattering parameters of the overall antenna-environment-antenna system. The solutions for S_{11} and S_{21} are given in (1) and (2), respectively. Solutions for S_{22} and S_{12} may be determined from (1) and (2) by interchanging "1" and "2" in the subscripts.

$$S_{11} = \Gamma_1 + \mathbf{R}_1\left[\mathbf{S}^e_{11} + \mathbf{S}^e_{12}\mathbf{S}_2\underbrace{\left(\mathbf{I} - \mathbf{S}^e_{22}\mathbf{S}_2\right)^{-1}}_{\mathrm{B}}\mathbf{S}^e_{21}\right] \cdot \underbrace{\left(\mathbf{I} - \mathbf{S}_1\left[\mathbf{S}^e_{11} + \mathbf{S}^e_{12}\mathbf{S}_2\left(\mathbf{I} - \mathbf{S}^e_{22}\mathbf{S}_2\right)^{-1}\mathbf{S}^e_{21}\right]\right)^{-1}}_{\mathrm{C}}\mathbf{T}_1 \quad (1)$$

$$S_{21} = \mathbf{R}_2\underbrace{\left[\mathbf{I} - \left(\mathbf{I} - \mathbf{S}^e_{22}\mathbf{S}_2\right)^{-1}\mathbf{S}^e_{21}\left(\mathbf{I} - \mathbf{S}_1\mathbf{S}^e_{11}\right)^{-1}\mathbf{S}_1\mathbf{S}^e_{12}\mathbf{S}_2\right]^{-1}}_{\mathrm{C}} \cdot \underbrace{\left(\mathbf{I} - \mathbf{S}^e_{22}\mathbf{S}_2\right)^{-1}}_{\mathrm{B}}\mathbf{S}^e_{21}\underbrace{\left(\mathbf{I} - \mathbf{S}_1\mathbf{S}^e_{11}\right)^{-1}}_{\mathrm{A}}\mathbf{T}_1. \quad (2)$$

In (1) and (2), we have also identified three different types of multiple scattering terms that are associated with feedback in the signal flow graph. These terms have the following physical interpretation.

- A: Multiple scattering between antenna #1 and the environment.
- B: Multiple scattering between antenna #2 and the environment.
- C: Multiple "round trip" scattering between antenna #1, the environment, and antenna #2.

III. Environment Scattering Parameter Matrices

The previous sections demonstrated the utility of the environment scattering parameter matrices $\mathbf{S}^e_{uv}$ in succinctly describing antenna coupling for arbitrary environments. In this section, we develop a mathematical description of $\mathbf{S}^e_{uv}$ by way of the environment's response to an outward propagating spherical modal excitation. We proceed by first determining the en-

[1]The process is analogous to the more common scalar signal flow graph manipulations described in [21], except that care must be taken with the order of the noncommutative matrix products.

vironment's *impedance* parameter matrices, denoted $\mathbf{Z}^e_{uv}$, and then calculating the environment's corresponding *scattering* parameter matrices $\mathbf{S}^e_{uv}$. This is convenient because whereas $\mathbf{Z}^e_{uv}$ is defined when all unexcited ports to be open-circuited, $\mathbf{S}^e_{uv}$ is defined when all ports are terminated in a nonreflecting load [22]. For spherical waves propagating into and out of radiation ports, the open-circuit condition corresponds to free space, and the nonreflecting load condition corresponds to a canonical minimum scattering antenna, as described in [23], [24]. In terms of setting up the problem, the free-space termination condition is inherently less complex than specifying minimum scattering antennas at all radiation ports. Here, we use the term "free space" to describe a scatterer-free space that is isotropic and homogeneous with a permittivity and permeability matching its surroundings. It is assumed that the antenna scattering parameters are calculated when the antennas are placed within an equivalent "free space".

We begin by reviewing relevant properties of spherical waves. Then, we describe the environment's total field due to a spherical modal excitation and determine a spherical wave expansion of this total field. Next, we relate the modal coefficients of the expansions to the elements of the impedance parameter matrices $\mathbf{Z}^e_{uv}$. Finally, we convert the impedance parameter matrices to the desired scattering parameter matrices $\mathbf{S}^e_{uv}$.

A. Spherical Waves

Following the conventions of [6] with the substitution $i = -j$, we denote a vector spherical wave of mode $\{s, m, n\}$ and type c, as $\mathbf{F}^{(c)}_{smn}(r, \theta, \phi)$, where r, θ, and ϕ denote the radial distance, zenith angle, and azimuth angle, respectively, of the spherical coordinate system. For the sake of brevity, we omit a mathematical definition of $\mathbf{F}^{(c)}_{smn}(r, \theta, \phi)$; see [6] for a rigorous definition. As in [6], we will generally favor a simplified single index mode notation for spherical waves whereby the index ℓ denotes the triple index $\{s, m, n\}$ such that $\mathbf{F}^{(c)}_{smn}(r, \theta, \phi) = \mathbf{F}^{(c)}_{\ell}(r, \theta, \phi)$. The index $c = 1, \ldots, 4$ denotes the type of spherical wave; here, we make use of outward propagating waves ($c = 3$), inward propagating waves ($c = 4$), and standing waves ($c = 1$). These waves are related by the following equality:

$$\mathbf{F}^{(1)}_{\ell}(r, \theta, \phi) = \frac{1}{2}\left[\mathbf{F}^{(3)}_{\ell}(r, \theta, \phi) + \mathbf{F}^{(4)}_{\ell}(r, \theta, \phi)\right]. \quad (3)$$

The electric field corresponding to a given spherical wave is given by [6]

$$\mathbf{E}^{(c)}_{\ell}(\mathbf{r}) = k\sqrt{\zeta}\mathbf{F}^{(c)}_{\ell}(r, \theta, \phi) \quad (4)$$

where $\mathbf{r} = (r, \theta, \phi)$ is the observation point in spherical coordinates, k is the wavenumber of the time-harmonic field, and $\zeta = \sqrt{\mu/\epsilon}$ denotes the wave impedance of the dielectric medium having permeability μ and permittivity ϵ.

Within a source-free, isotropic, and homogeneous region that contains the origin, an arbitrary time-harmonic electric field $\mathbf{E}(\mathbf{r})$ of wavenumber k may be expanded as a weighted summation of standing ($c = 1$) spherical waves according to

$$\mathbf{E}(\mathbf{r}) = k\sqrt{\zeta}\sum_{\ell} w^{(1)}_{\ell}\mathbf{F}^{(1)}_{\ell}(r, \theta, \phi). \quad (5)$$

The modal coefficients $w^{(1)}_{\ell}$ may be determined from observations of $\mathbf{E}(\mathbf{r})$ along a bounding spherical interface Ω. Assuming Ω is centered about the origin with a radius A, the resulting coefficients are given by [6]

$$w^{(1)}_{\ell} = \frac{1}{k\sqrt{\zeta}}\frac{(-1)^m}{\tilde{R}_{sn}(kA)}\int_{\Omega}\mathbf{E}(A, \theta, \phi)\cdot\mathbf{F}^{(1)}_{\ell^{\dagger}}(A, \theta, \phi)\, d\Omega \quad (6)$$

where $\ell^{\dagger} = \{s, -m, n\}$ denotes the mode index used to extract the ℓth mode's coefficient; $\tilde{R}_{sn}(x)$ is given by

$$\tilde{R}_{sn}(x) = \begin{cases} [j_n(x)]^2, & \text{for } s = 1 \\ \left[\frac{1}{x}\frac{d}{dx}(x\, j_n(x))\right]^2 + n(n+1)\left[\frac{j_n(x)}{x}\right]^2, & \text{for } s = 2 \end{cases} \quad (7)$$

and $j_n(x)$ denotes the nth order spherical Bessel function of the first kind.

B. Electric Field due to a Spherical Modal Excitation

Consider the total field at some observation point $\mathbf{r}$ due to a source centered about $\mathbf{r}'$ and radiating a single spherical wave of mode ℓ' into an arbitrary environment. Using conventional electric field formulations based on dyadic Green's functions (see [25]), we define this total field, denoted $\mathbf{E}^e_{\ell'}(\mathbf{r}|\mathbf{r}')$, as

$$\mathbf{E}^e_{\ell'}(\mathbf{r}|\mathbf{r}') = -j\zeta k\int\overline{\mathbf{G}}^e(\mathbf{r}|\mathbf{r}_0)\cdot\mathbf{J}_{\ell'}(\mathbf{r}_0 - \mathbf{r}')\, d\mathbf{r}_0 \quad (8)$$

where $\overline{\mathbf{G}}^e_{\ell'}(\mathbf{r}|\mathbf{r}')$ is the environment's electric dyadic Green's function, and $\mathbf{J}_{\ell'}(\mathbf{r})$ is a modal current density characterized by the following properties:

$$\mathbf{J}_{\ell'}(\mathbf{r}) = 0, \quad \text{for } \|\mathbf{r}\| \geq A \quad (9)$$

and

$$-j\zeta k\int\overline{\mathbf{G}}^{\mathrm{FS}}(\mathbf{r}|\mathbf{r}_0)\cdot\mathbf{J}_{\ell'}(\mathbf{r}_0)\, d\mathbf{r}_0 = k\sqrt{\zeta}\mathbf{F}^{(3)}_{\ell'}(r, \theta, \phi), \quad \text{for } \|\mathbf{r}\| \geq A. \quad (10)$$

In (10), $\overline{\mathbf{G}}^{\mathrm{FS}}(\mathbf{r}|\mathbf{r}')$ is the free-space (i.e., infinite scatterer-free space) electric dyadic Green's function. The current density $\mathbf{J}_{\ell'}(\mathbf{r}')$ defines the excitation for a unit amplitude outward propagating ($c = 3$) spherical wave of mode ℓ'. For arbitrary ℓ', analytic representations for $\mathbf{J}_{\ell'}(\mathbf{r}')$ have been presented in the literature [26], [27]. As a special case of (8), we define $\mathbf{E}^{\mathrm{FS}}_{\ell'}(\mathbf{r}|\mathbf{r}')$ as the total field arising when this modal current source is located at $\mathbf{r}'$ in free-space

$$\mathbf{E}^{\mathrm{FS}}_{\ell'}(\mathbf{r}|\mathbf{r}') = -j\zeta k\int\overline{\mathbf{G}}^{\mathrm{FS}}(\mathbf{r}|\mathbf{r}_0)\cdot\mathbf{J}_{\ell'}(\mathbf{r}_0 - \mathbf{r}')\, d\mathbf{r}_0. \quad (11)$$

Note that in (8)–(11), we have used superscripts to distinguish between Green's functions and total field response functions for the arbitrary environment ("e") and free space ("FS").

C. Spherical Wave Expansion of the Electric Field Due to a Spherical Modal Excitation

We consider spherical wave expansions of $\mathbf{E}^e_{\ell'}(\mathbf{r}|\mathbf{r}')$ for two configurations relevant to our determination of $\mathbf{Z}^e_{uv}$: 1) when $\mathbf{r}'$

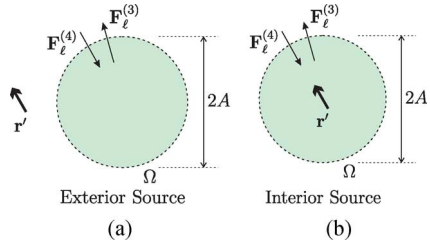

Fig. 2. Two scenarios for determining the environment's impedance parameter matrices $\mathbf{Z}^e_{uv}$. (a) Source at $\mathbf{r}'$ exterior to the bounding sphere Ω. (b) Source interior to and centered within Ω at $\mathbf{r}' = \mathbf{0}$. For both scenarios, the coordinate system's origin coincides with the center of the bounding spherical interface Ω.

(the origin of the spherical wave) is exterior to Ω, and 2) when $\mathbf{r}'$ is centered within and bounded by Ω. We assume that the spherical interface Ω has a radius A and bounds a homogeneous and isotropic volume. For convenience, we will also assume that Ω is centered about the origin. Fig. 2 illustrates the problem geometry for the two cases.

1) Exterior Source: For the exterior source problem, $\mathbf{E}^e_{\ell'}(\mathbf{r}|\mathbf{r}')$ is source-free within Ω. This allows the total field $\mathbf{E}^e_{\ell'}(\mathbf{r}|\mathbf{r}')$ on Ω to be expanded as a weighted summation of spherical standing waves ($c = 1$)

$$\mathbf{E}^e_{\ell'}(\mathbf{r}|\mathbf{r}')|_{\mathbf{r}\in\Omega} = k\sqrt{\zeta}\sum_\ell w_\ell^{(1)}\mathbf{F}_\ell^{(1)}(A,\theta,\phi) \tag{12}$$

where $w_\ell^{(1)}$ denotes the complex coefficients for each of the standing waves. Using (6), the modal coefficients for the exterior source problem are given by

$$w_\ell^{(1)} = \frac{1}{k\sqrt{\zeta}}\frac{(-1)^m}{\tilde{R}_{sn}(kA)}\int_\Omega \mathbf{E}^e_{\ell'}(A,\theta,\phi|\mathbf{r}')\cdot\mathbf{F}^{(1)}_{\ell^\dagger}(A,\theta,\phi)\,d\Omega. \tag{13}$$

2) Interior Source: For the interior source problem, $\mathbf{E}^e_\ell(\mathbf{r}|\mathbf{r}')$ for $\mathbf{r}\in\Omega$ may be described by a superposition of standing waves ($c = 1$) plus a single outward propagating wave ($c = 3$). Thus, for an interior source centered about the origin

$$\mathbf{E}^e_{\ell'}(\mathbf{r}|\mathbf{0})|_{\mathbf{r}\in\Omega} = \mathbf{E}^{\mathrm{FS}}_{\ell'}(\mathbf{r}|\mathbf{0})|_{\mathbf{r}\in\Omega} + k\sqrt{\zeta}\sum_\ell w_\ell^{(1)}\mathbf{F}_\ell^{(1)}(A,\theta,\phi) \tag{14}$$

where we have isolated the source's free-space contribution using the free-space electric field modal response function defined in (11). By removing this free-space contribution and then applying (6), the modal coefficients are given by

$$w_\ell^{(1)} = \frac{1}{k\sqrt{\zeta}}\frac{(-1)^m}{\tilde{R}_{sn}(kA)} \times\int_\Omega\left[\mathbf{E}^e_{\ell'}(A,\theta,\phi|\mathbf{0}) - \mathbf{E}^{\mathrm{FS}}_{\ell'}(A,\theta,\phi|\mathbf{0})\right]\cdot\mathbf{F}^{(1)}_{\ell^\dagger}(A,\theta,\phi)\,d\Omega. \tag{15}$$

D. Solution for the Impedance Parameter Matrices, $\mathbf{Z}^e_{uv}$

The expansions coefficients $w_\ell^{(1)}$ in (13) and (15) describe the environment's response to a modal excitation for free-space termination conditions. Recognizing that the excitation corresponds to an outward propagating wave with a coefficient of unity, the coefficients $w_\ell^{(1)}$, along with the radiation ports' characteristic impedances, lead directly to the self- and mutual-impedances of the environment.

Combining (13) and (15), and recognizing that the exterior and interior source problems correspond to $u \neq v$ and $u = v$, respectively, the environment's impedance parameter matrices are given by

$$\mathbf{Z}^e_{uv} = \mathbf{Z}^{1/2}_{0,u}\left[2\tilde{\mathbf{Z}}^e_{uv} + \mathbf{I}\right]\mathbf{Z}^{1/2}_{0,v} \tag{16}$$

where the elements of $\tilde{\mathbf{Z}}^e_{uv}$ are given by (18), shown at the bottom of the page, and $\mathbf{Z}_{0,i}$ is a diagonal matrix of complex characteristic impedances whose pth diagonal element is

$$\mathbf{Z}_{0,i}|_{(p,p)} = Z^{(i)}_{0,\ell_p} \tag{17}$$

where $Z^{(i)}_{0,\ell_p}$ is the characteristic impedance of the ith spherical interface's pth radiation port of mode ℓ_p.

In (18), $\tilde{\mathbf{Z}}^e_{uv}\Big|_{(p,q)}$ is associated with the standing wave of mode $\ell_p = \{s_p, m_p, n_p\}$ at the uth antenna's bounding spherical interface Ω_u arising due to an excitation of mode $\ell_q = \{s_q, m_q, n_q\}$ originating at the vth antenna's bounding spherical interface Ω_v, $\ell_p^\dagger = \{s_p, -m_p, n_p\}$ is the mode used to extract the standing wave of mode ℓ_p, and the coordinate system's origin is assumed to be centered within the spherical interface Ω_u, which bounds and is nominally centered about the uth antenna (i.e., $\mathbf{r}_u = \mathbf{0}$). Due to the factor of one-half in (18), $\tilde{\mathbf{Z}}^e_{uv}$ relate outward propagating waves originating at the vth antenna to inward propagating waves incident on the uth antenna (for free-space termination conditions). In Section IV, we use this physical interpretation of $\tilde{\mathbf{Z}}^e_{uv}$ to formulate an alternative set of antenna coupling equations analogous to those used in spherical near-field antenna measurements.

E. Solution for the Scattering Parameter Matrices, $\mathbf{S}^e_{uv}$

Using (16) and the impedance-to-scattering parameter matrix transformation described in Appendix A, the environment scattering parameters are given by:

$$\mathbf{S}^e_{uv} = (\mathbf{U}_u\mathbf{Z}^{1/2}_{0,u})\tilde{\mathbf{S}}^e_{uv}(\mathbf{U}_v\mathbf{Z}^{1/2}_{0,v})^{-1} \tag{19}$$

where $\mathbf{U}_i$ is a diagonal matrix whose pth diagonal element is

$$\mathbf{U}_i|_{(p,p)} = \frac{\sqrt{\mathrm{Re}\left\{Z^{(i)}_{0,\ell_p}\right\}}}{2|Z^{(i)}_{0,\ell_p}|} \tag{20}$$

$$\tilde{\mathbf{Z}}^e_{uv}\Big|_{(p,q)} = \frac{1}{2}\frac{1}{k\sqrt{\zeta}}\frac{(-1)^{m_p}}{\tilde{R}_{s_p n_p}(kA)}\begin{cases}\int_{\Omega_u}\mathbf{E}^e_{\ell_q}(A,\theta,\phi|\mathbf{r}_v)\cdot\mathbf{F}^{(1)}_{\ell_p^\dagger}(A,\theta,\phi)\,d\Omega_u, & \text{for } u\neq v\\ \int_{\Omega_u}\left[\mathbf{E}^e_{\ell_q}(A,\theta,\phi|\mathbf{r}_v) - \mathbf{E}^d_{\ell_q}(A,\theta,\phi|\mathbf{r}_v)\right]\cdot\mathbf{F}^{(1)}_{\ell_p^\dagger}(A,\theta,\phi)\,d\Omega_u, & \text{for } u = v\end{cases}. \tag{18}$$

and $\tilde{\mathbf{S}}^e_{uv}$ is an auxiliary matrix that is related to $\tilde{\mathbf{Z}}^e_{uv}$ by

$$\tilde{\mathbf{S}}^e = \tilde{\mathbf{Z}}^e(\tilde{\mathbf{Z}}^e + \mathbf{I})^{-1}. \tag{21}$$

In (21), $\tilde{\mathbf{S}}^e$ and $\tilde{\mathbf{Z}}^e$ are block matrices given by

$$\tilde{\mathbf{Z}}^e = \begin{bmatrix} \tilde{\mathbf{Z}}^e_{11} & \tilde{\mathbf{Z}}^e_{12} \\ \tilde{\mathbf{Z}}^e_{21} & \tilde{\mathbf{Z}}^e_{22} \end{bmatrix} \tag{22}$$

$$\tilde{\mathbf{S}}^e = \begin{bmatrix} \tilde{\mathbf{S}}^e_{11} & \tilde{\mathbf{S}}^e_{12} \\ \tilde{\mathbf{S}}^e_{21} & \tilde{\mathbf{S}}^e_{22} \end{bmatrix}. \tag{23}$$

In the following section, we show how the environment scattering parameter decomposition given in (19) leads to a simplification of the coupling equations presented in (1)–(2) that are compatible with the classically-defined antenna scattering parameters.

IV. Alternative Coupling Formulations

A. "Far-Field" Formulation

As discussed in Appendix A, the antenna scattering parameters allow for a decomposition similar to (19); specifically[2]

$$\Gamma_i = \left(U_0 Z_0^{1/2}\right) \tilde{\Gamma}_i \left(U_0 Z_0^{1/2}\right)^{-1} \tag{24a}$$

$$\mathbf{T}_i = \left(U_0 Z_0^{1/2}\right) \tilde{\mathbf{T}}_i \left(\mathbf{U}_i \mathbf{Z}_{0,i}^{1/2}\right)^{-1} \tag{24b}$$

$$\mathbf{R}_i = \left(\mathbf{U}_i \mathbf{Z}_{0,i}^{1/2}\right) \tilde{\mathbf{R}}_i \left(U_0 Z_0^{1/2}\right)^{-1} \tag{24c}$$

$$\mathbf{S}_i = \left(\mathbf{U}_i \mathbf{Z}_{0,i}^{1/2}\right) \tilde{\mathbf{S}}_i \left(\mathbf{U}_i \mathbf{Z}_{0,i}^{1/2}\right)^{-1} \tag{24d}$$

where U_0 and Z_0 are scalar analogs of the diagonal matrices $\mathbf{U}_i$ and $\mathbf{Z}_{0,i}$ but defined in terms of the characteristic impedances of the antennas' physical ports (i.e., Ports #1 and #2 in Fig. 1). As discussed in Appendix A, (24)'s decomposition relates an antenna's so-called "near-field" scattering parameters (Γ_i, $\mathbf{T}_i$, $\mathbf{R}_i$, and $\mathbf{S}_i$) defined at a *finite*-radius spherical interface to so-called "far-field" scattering parameters ($\tilde{\Gamma}_i$, $\tilde{\mathbf{T}}_i$, $\tilde{\mathbf{R}}_i$, and $\tilde{\mathbf{S}}_i$) defined at an *infinite*-radius spherical interface. The "near-field" antenna (and environment) scattering parameters correspond to those described in Section II, whereas the "far-field" antenna scattering parameters are exactly those used in classical spherical modal descriptions of radiating and scattering structures.

When the "near-field" antenna and environment scattering parameter matrix decompositions are substituted into the coupling (1)–(2), the diagonal matrices $\mathbf{U}_i \mathbf{Z}_{0,i}^{1/2}$ and the scalar $U_0 Z_0^{1/2}$ will cancel[3] with their associated inverses. This leads to an equivalent coupling formulation expressed in terms of the "far-field" antenna and environment scattering parameters. The associated coupling equations may be attained by performing the following substitutions on (1) and (2):

$$\Gamma_i \rightarrow \tilde{\Gamma}_i \tag{25a}$$

$$\mathbf{T}_i \rightarrow \tilde{\mathbf{T}}_i \tag{25b}$$

$$\mathbf{R}_i \rightarrow \tilde{\mathbf{R}}_i \tag{25c}$$

$$\mathbf{S}_i \rightarrow \tilde{\mathbf{S}}_i \tag{25d}$$

$$\mathbf{S}^e_{uv} \rightarrow \tilde{\mathbf{S}}^e_{uv}. \tag{25e}$$

Coupling equations based on (1)–(2) with the substitutions indicated by (25) allow for direct substitution of the classically-defined "far-field" antenna scattering parameters.

B. "Open-Circuit" Formulation

The matrices $\tilde{\mathbf{Z}}^e_{uv}$ describe the reflection and transmission of spherical waves under free-space termination conditions. This provides a classical scattering matrix description of the environment that aligns with the physical interpretation of the transmission/translation matrices used in free-space antenna coupling formulations (e.g., [6]) while also allowing for use of the "far-field" antenna scattering parameters. These observations suggest that an alternative, albeit equivalent, antenna coupling formulation may be attained by performing the following substitutions on (1) and (2):

$$\Gamma_i \rightarrow \tilde{\Gamma}_i \tag{26a}$$

$$\mathbf{T}_i \rightarrow \tilde{\mathbf{T}}_i \tag{26b}$$

$$\mathbf{R}_i \rightarrow \tilde{\mathbf{R}}_i \tag{26c}$$

$$\mathbf{S}_i \rightarrow \tilde{\mathbf{S}}_i - \mathbf{I} \tag{26d}$$

$$\mathbf{S}^e_{uv} \rightarrow \tilde{\mathbf{Z}}^e_{uv}. \tag{26e}$$

Coupling equations based on (1)–(2) with the substitutions indicated by (26) may be interpreted as extensions to the classic coupling equations used in free-space antenna and electro-acoustic transducer characterizations [2], [6], [28].

V. Numerical Simulations

In the following sections, we present example numerical results for our formulation for the case of z-polarized infinitesimal electric dipole antennas in free space and an ideal rectangular cavity. Our numerical simulations were based on the alternative formulation described in Section IV-B. The integral appearing in (18) was evaluated by use of first-order linear spherical interpolation/integration (see [29], [30]) of observations $\mathbf{r}$ on a 12-point icosahedral mesh lying on a spherical interface of radius $A = \lambda_0/10$. Note that, because the simulations used z-polarized infinitesimal electric dipoles, we only had to consider a single spherical mode $\{s = 2, m = 0, n = 1\}$. As a partial validation of our formulation, we compared numerical results to those obtained from environment-specific calculations of the antennas' self- and mutual impedance by use of the induced EMF method [31, Chapter 7]. As in [32], the environment-specific calculations of the dipoles' self- and mutual impedances were determined from the environment's electric dyadic Green's function.

A. Free-Space Environment

The problem geometry for the free-space environment is illustrated in Fig. 3. Two lossless and perfectly matched z-polarized infinitesimal electric dipoles are positioned on the x-axis within a free-space environment and separated by a distance d.

[2]Note that $\Gamma_i = \tilde{\Gamma}_i$, whereby the antenna's reflection coefficient is unaffected by the specification of the radiation ports' spherical interface as may be expected.

[3]The scalar $U_0 Z_0^{1/2}$ cancels because we have specified the characteristic impedances of the two antenna ports to be identical.

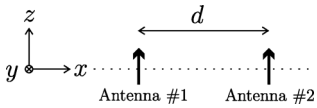

Fig. 3. Diagram of the free-space environment test case.

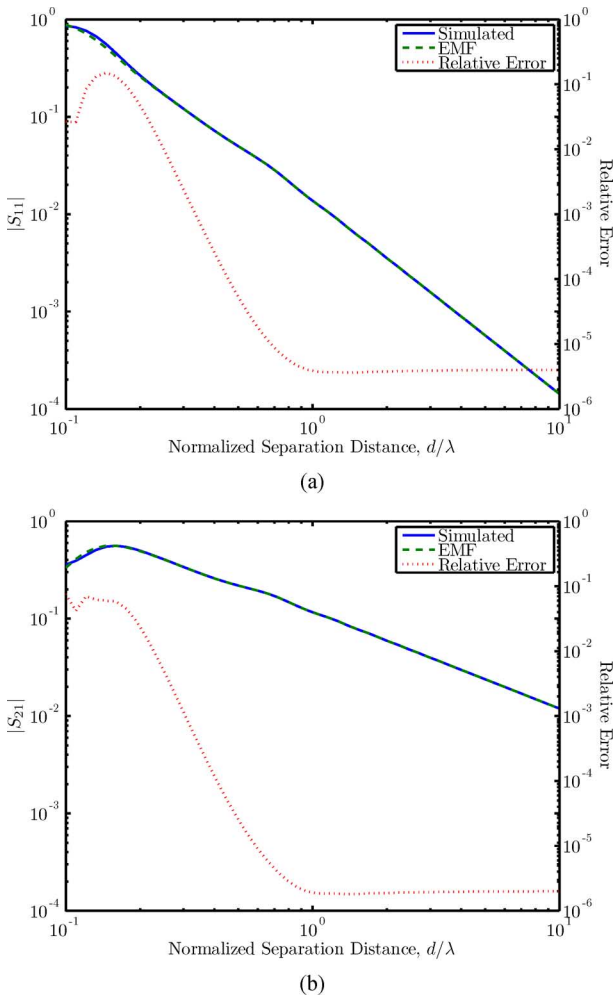

Fig. 4. Comparison of the simulated and analytic scattering parameters for two perfectly matched z-polarized infinitesimal electric dipoles on the x-axis separated by a distance d: (a) S_{11} and (b) S_{21}.

Fig. 4 compares the simulation's antenna port scattering parameters, S_{11} and S_{21}, with those computed by way of the EMF method for $d \in [0.1\lambda, 10\lambda]$. The dotted lines indicate the relative error in the simulated scattering parameters is approximately constant and less that 10^{-5} for $\lambda \leq d \leq 10\lambda$. Repeated simulations with smaller bounding spherical interfaces resulted in even smaller relative errors for all d. Similar error reductions were obtained by increasing the number of observation points on the bounding spherical interface. This indicated that the relative error was dominated by the accuracy of the numerical implementation of (18) as might be expected.

B. Rectangular Cavity Environment

The geometry of the rectangular cavity test environment is illustrated in Fig. 5. Two lossless and perfectly matched

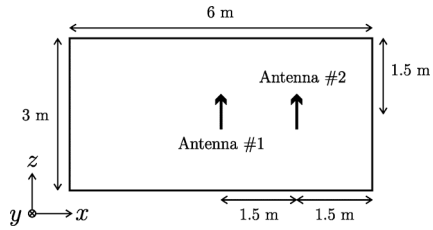

Fig. 5. Diagram of the 3-D rectangular cavity test case corresponding to a slice in the x-z plane containing the two z-polarized dipoles. The two antennas were centered with respect to the y dimension of the cavity, which spanned 7 m.

z-polarized infinitesimal electric dipoles were positioned in a 6 m$\times$7 m$\times$3 m lossless rectangular cavity with perfectly electrically conducting walls. The first antenna was centered within the cavity, and the second antenna was positioned 1.5 m from the first antenna along the x-direction. The implementation of the rectangular cavity dyadic Green's function was based on the computationally efficient representations described in [33].

Fig. 6 compares the simulation's antenna port scattering parameters, S_{11}, S_{22}, and S_{21}, with those computed by way of the EMF method for frequencies ranging from 100 MHz to 1 GHz. The relative error for the rectangular cavity test case fluctuates around 10^{-5}. As in Fig. 4, the relative errors in Fig. 6 were dominated by the accuracy of the numerical implementation of (18). The variations in this error are attributed to the rapid variations in the values of S_{11}, S_{22}, and S_{21} due to the cavity's resonances.

VI. Applications

The coupling equations given by (1)–(2), along with the alternative formulations presented in Section IV, provide a framework for analyzing antenna coupling in arbitrary environments. In the following, we discuss the pros and cons of two possible applications of this framework: electromagnetic simulations and analytic analysis. In a forthcoming paper [34], we demonstrate the utility of this framework for analytic analysis by deriving the spatial autocovariance of scattering parameters measured in a reverberation chamber.

A. Electromagnetic Simulations

As demonstrated by the numerical validation in Section V, the coupling equations may be used to conduct full-wave electromagnetic simulations of antennas in different environments. The advantage of such a solver lies in the decomposition of the overarching coupling problem into independent calculations of the scattering parameter matrices for the antennas and environment. Thereby, a given environment only needs to be characterized (in terms of impedance or scattering parameter matrices) once; thereafter, antenna coupling may be rapidly computed for any pair of known antennas in that environment. However, the antenna's bistatic scattering matrices $\mathbf{S}_i$ are rarely known, and determining $\mathbf{S}_i$ numerically or experimentally is extremely time-consuming [8], [35]–[38]. Numerically calculating the electric field due to a modal excitation, $\mathbf{E}^e_{\ell'}(\mathbf{r}|\mathbf{r}')$ defined in (8), is also computationally expensive. For these reasons, extending the simulation setup described in Section V to more realistic antennas may not be worth the effort.

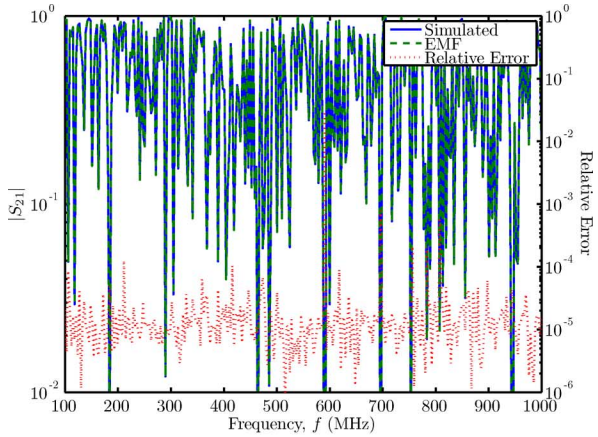

(a)

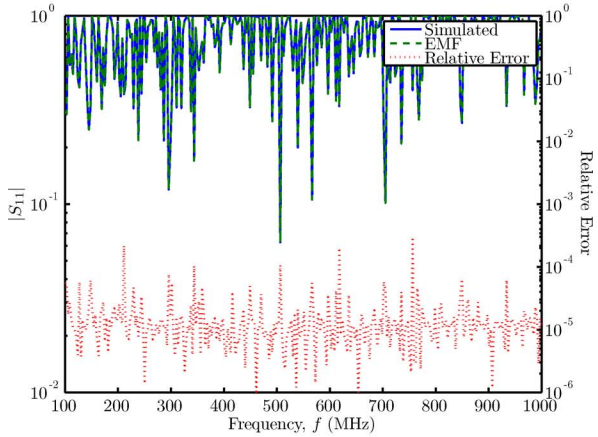

(b)

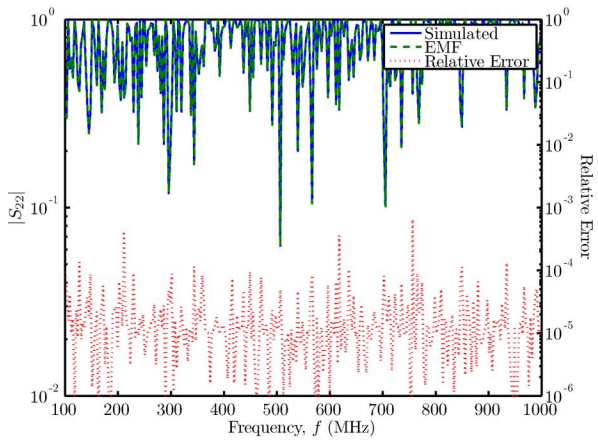

(c)

Fig. 6. Comparison of the simulated and analytic scattering parameters for a pair of z-polarized perfectly matched infinitesimal electric dipoles: (a) S_{21}, (b)S_{11}, and (c) S_{22}.

The situation improves somewhat when considering more complex scattering environments that allow for a statistical description of $\mathbf{S}^e_{uv}$ or $\mathbf{Z}^e_{uv}$. This could be useful for numerically investigating the coupling between two antennas inside of a reverberant cavity (e.g., a reverberation chamber). The availability of statistical models for the impedance and scattering parameter matrices for reverberant cavities (see [39]–[42]) eliminates the need to compute $\mathbf{E}^e_{\ell'}(\mathbf{r}|\mathbf{r}')$. However, the computational effort required to determine the antennas' bistatic scattering matrices $\mathbf{S}_i$ must still be considered.

B. Analytic Analysis

The framework also enables analytic investigations of antenna coupling. For example, by nature of the spherical wave formulation considered here, the framework enables a closed-form analytic solution to antenna coupling for the spherical cavity environment. This could serve as a canonical reference environment for studying antenna coupling in arbitrary reverberant cavities. Simplifications are possible with additional knowledge of the antennas and/or environment (e.g., reciprocity and passivity). For example, by following the antenna reciprocity proof in [6], it may be shown that for a reciprocal environment

$$\tilde{\mathbf{Z}}^e_{uv}\big|_{(\ell_p,\ell_q)} = (-1)^{m_p+m_q}\tilde{\mathbf{Z}}^e_{vu}\big|_{(\ell^\dagger_q,\ell^\dagger_p)}. \tag{27}$$

Equation (27)'s notation follows that used in (18) with the additional mode index $\ell^\dagger_q = \{s_q, -m_q, n_q\}$. Combining environment and antenna reciprocity with the reciprocity constraint that $S_{21} = S_{12}$ or, alternatively, combining lossless environments and antennas with the energy constraint that $|S_{21}|^2 + |S_{11}|^2 = 1$ may lead to further simplifications that elucidate the underlying physical constraints of certain scattering and propagation problems.

Approximations to the coupling equations are possible when antenna-antenna and antenna-environment interactions are weak and dominated by first-order antenna/environment scattering. When valid, the multiple scattering terms of the form $(\mathbf{I}-\mathbf{A})^{-1}$ in the coupling equations may be approximated as [43]

$$(\mathbf{I}-\mathbf{A})^{-1} \approx \mathbf{I}+\mathbf{A} \tag{28}$$

provided $\|\mathbf{A}\| \ll 1$ where $\|\cdot\|$ denotes the matrix norm. In a forthcoming paper [34], we demonstrate how (28) may be used to simplify the coupling equations for the case of a lossy reverberation chamber. This simplified coupling model is combined with a statistical description of the environment to derive the spatial autocovariance of S-parameters measured in a lossy reverberation chamber.

VII. Summary

This work presented a rigorous framework for analyzing coupling between antennas in arbitrary environments. The framework decomposes the coupling problem into antenna and environment terms that may be characterized independently of each other. Three equivalent formulations were presented. In the first formulation, the environment was characterized for the case of nonreflecting loads at the environment's radiation ports defined at finite-radii spherical interfaces. Simplification of this formulation resulted in a secondary formulation that is compatible with classically-defined antenna scattering parameter matrices. The third formulation used an environment description that shares the same physical interpretation as the transmission/translation matrices used in conventional spherical near-field antenna coupling formulations. The formulations provide a framework for investigating deterministic and stochastic coupling between antennas in canonical and complex environments, respectively.

APPENDIX
RELATIONSHIP BETWEEN IMPEDANCE AND SCATTERING PARAMETER MATRICES

Characteristic Impedance of a Radiation Port: For an origin-centered and unit amplitude outward propagating spherical wave of mode $\ell = \{s, m, n\}$, the complex power traversing a spherical interface Ω of radius A centered about the origin is (cf. [6, eq. (2.43)–(2.53)])

$$p_{0,\ell} = -\frac{j|kA|^2}{2}\int_{\Omega}\left[\mathbf{F}^{(3)}_{smn}(A,\theta,\phi)\times\mathbf{F}^{(3)*}_{3-s,m,n}(A,\theta,\phi)\right]\cdot\hat{\mathbf{r}}\,d\Omega. \tag{29}$$

In general, $p_{0,\ell}$ is complex. However, it may be shown that $p_{0,\ell}\to(1/2)e^{2\mathrm{Im}\{k\}A}$ as $A\to\infty$ whereby $p_{0,\ell}$ is purely real.

The corresponding radiation port's characteristic impedance $Z_{0,\ell}$ at the interface Ω may be defined in terms of a pair of voltage- and current-like quantities $i_{0,\ell}$ and $v_{0,\ell}$ such that [44]

$$Z_{0,\ell} = \frac{v_{0,\ell}}{i_{0,\ell}} \tag{30}$$

with the constraint that

$$p_{0,\ell} = \frac{1}{2}v_{0,\ell}i^*_{0,\ell}. \tag{31}$$

This representation allows for a fair amount of freedom in the specification of either $v_{0,\ell}$ or $i_{0,\ell}$. For convenience, we specify that $v_{0,\ell}$ be purely real. Note that $\angle Z_{0,\ell} = \angle p_{0,\ell}$.

Fundamental Relationship: Suppose a multiport system with impedance parameter matrix $\mathbf{Z}$ relating currents to voltages at each port. The corresponding scattering parameter matrix description of this system, defined with respect to the ports' characteristic impedances, is given by [44]

$$\mathbf{S} = \mathbf{U}(\mathbf{Z}-\mathbf{Z}_0)(\mathbf{Z}+\mathbf{Z}_0)^{-1}\mathbf{U}^{-1} \tag{32}$$

where $\mathbf{Z}_0$ is a diagonal matrix of potentially complex characteristic impedances and $\mathbf{U}$ is a diagonal matrix of coefficients that map voltages to wave amplitudes. The pth diagonal element of $\mathbf{Z}_0$ corresponds to the characteristic impedance Z_{0,ℓ_p} of the pth port's mode ℓ_p, and the pth diagonal element of $\mathbf{U}$ is given by[4]

$$\mathbf{U}|_{(p,p)} = \frac{\sqrt{\mathrm{Re}\{Z_{0,\ell_p}\}}}{2|Z_{0,\ell_p}|}. \tag{33}$$

An Impedance Parameter Matrix Decomposition: Consider an impedance parameter matrix decomposition

$$\mathbf{Z} = \mathbf{Z}_0^{1/2}[2\tilde{\mathbf{Z}}+\mathbf{I}]\mathbf{Z}_0^{1/2} \tag{34}$$

analogous to that used in (16). Substituting (34) into (32) and rearranging terms yields

$$\mathbf{S} = \left(\mathbf{U}\mathbf{Z}_0^{1/2}\right)\tilde{\mathbf{Z}}(\tilde{\mathbf{Z}}+\mathbf{I})^{-1}\left(\mathbf{U}\mathbf{Z}_0^{1/2}\right)^{-1}. \tag{35}$$

[4]Our representation of $\mathbf{U}$ is a simplification of that presented in [44], because we have required that $v_{0,\ell}$ be purely real

"Near-Field" and "Far-Field" Scattering Parameters: For the case of purely real characteristic impedances, $\mathbf{U}\mathbf{Z}_0^{1/2} = (1/2)\mathbf{I}$ and (35) becomes

$$\tilde{\mathbf{S}} = \tilde{\mathbf{Z}}(\tilde{\mathbf{Z}}+\mathbf{I})^{-1} \tag{36}$$

where we have modified our notation to distinguish (35) from (36) and be consistent with the preceding sections.

For spherical waves in a *lossless* medium, (36) defines the scattering parameter matrix when the radiation ports are defined on an infinite radius spherical interface such that $p_{0,\ell}$, and thereby $Z_{0,\ell}$, is purely real. This indicates that $\tilde{\mathbf{S}}$ is a scattering parameter matrix description of the system as observed in the far field. The diagonal matrix $\mathbf{U}\mathbf{Z}_0^{1/2}$ and its inverse provide a transformation between this "far-field" scattering parameter matrix $\tilde{\mathbf{S}}$ and (35)'s "near-field" scattering parameter matrix description $\mathbf{S}$, which is defined with respect to a finite radius spherical interface. For a lossy medium, this physical interpretation and the associated nomenclature breaks down, because an inward propagating wave originating at infinity requires infinite power. Regardless, (35)'s mathematical description of the scattering parameter matrix remains valid, and the "near-field" and "far-field" terminology is useful for distinguishing between $\mathbf{S}$ and $\tilde{\mathbf{S}}$, respectively.

ACKNOWLEDGMENT

The author acknowledges the helpful suggestions of Dr. R. H. Direen, Dr. K. A. Remley, Dr. R. C. Wittmann, and the reviewers.

REFERENCES

[1] D. M. Kerns, "Correction of near-field antenna measurements made with an arbitrary but known measuring antenna," *Electron. Lett.*, vol. 6, no. 11, pp. 346–347, May 1970.

[2] D. M. Kerns, *Plane-Wave Scattering-Matrix Theory of Antennas and Antenna-Antenna Interactions*. Boulder, CO: National Bureau of Standards, 1981, vol. 162, National Bureau of Standards Monograph.

[3] W. M. Leach Jr. and D. T. Paris, "Probe compensated near-field measurements on a cylinder," *IEEE Trans. Antennas Propag.*, vol. AP-21, no. 4, pp. 435–445, Jul. 1973.

[4] F. Jensen, "On the probe compensation for near-field measurements on a sphere," *Archiv Elektronik und Uebertragungstechnik*, vol. 29, pp. 305–308, Jul./Aug. 1975.

[5] R. C. Lewis, "Spherical-wave source-scattering matrix analysis of coupled antennas; A general system two-port solution," *IEEE Trans. Antennas Propag.*, vol. AP-35, no. 12, pp. 1375–1380, Dec. 1987.

[6] J. E. Hansen, Ed., *Spherical Near-Field Antenna Measurements*. London, U.K.: Peregrinus, 1988.

[7] J. E. B. J. D. T. Paris and W. M. Leach, "Basic theory of probe-compensated near-field measurements," *IEEE Trans. Antennas Propag.*, vol. AP-26, no. 3, pp. 373–379, May 1978.

[8] A. D. Yaghjian, "An overview of near-field antenna measurements," *IEEE Trans. Antennas Propag.*, vol. AP-34, no. 1, pp. 30–45, Jan. 1986.

[9] M. G. Cote and R. M. Wing, "Demonstration of bistatic electromagnetic scattering measurements by spherical near-field scanning," in *Proc. AMTA Symp.*, 1993, pp. 191–197.

[10] J. Rubio, M. A. González, and J. Zapata, "Generalized-scattering-matrix analysis of a class of finite arrays of coupled antennas by using 3-D FEM and spherical mode expansion," *IEEE Trans. Antennas Propag.*, vol. 53, no. 3, pp. 1133–1144 , Mar. 2005.

[11] J. Córcoles, J. Pontes, M. A. González, and T. Zwick, "Modelling line-of-sight coupled MIMO systems with generalized scattering matrices and spherical wave translations," *Electron. Lett.*, vol. 45, no. 12, pp. 598–599, Jun. 2009.

[12] P. C. Waterman, "Symmetry, unitarity, and geometry in electromagnetic scattering," *Phys. Rev. D*, vol. 3, no. 4, pp. 825–839, Feb. 1971.

[13] B. Peterson and S. Ström, "T matrix for electromagnetic scattering from an arbitrary number of scatterers and representations of $\mathrm{e}(3)$," *Phys. Rev. D*, vol. 8, no. 10, pp. 3661–3678, Nov. 1973.
[14] L. B. Felsen, M. Mongiardo, and P. Russer, "Electromagnetic field representations and computations in complex structures I: Complexity architecture and generalized network formulation," *Int. J. Numer. Model.: Electron. Netw., Devices, Fields*, vol. 15, no. 1, pp. 93–107, Jan./Feb. 2002.
[15] L. B. Felsen, M. Mongiardo, and P. Russer, "Electromagnetic field representations and computations in complex structures II: Alternative Green's functions," *Int. J. Numer. Model.: Electron. Netw., Devices, Fields*, vol. 15, no. 1, pp. 109–125, Jan./Feb. 2002.
[16] P. Russer, M. Mongiardo, and L. B. Felsen, "Electromagnetic field representations and computations in complex structures III: Network representations of the connection and subdomain circuits," *Proc. Int. J. Numer. Model.: Electron. Netw., Devices, Fields*, vol. 15, no. 1, pp. 127–145, Jan./Feb. 2002.
[17] E. Martini, G. Carli, and S. Maci, "A domain decomposition method based on a generalized scattering matrix formalism and a complex source expansion," *Progress Electromagn. Res. B*, vol. 19, pp. 445–473, 2010.
[18] C. D. Giovampaola, E. Martini, A. Toccafondi, and S. Maci, "Antenna mismatch induced by nearby scatterers through a spherical wave–Generalized scattering matrix approach," in *URSI Int. Symp. Electromagn. Theory*, Berlin, Germany, Aug. 16–19, 2010, pp. 776–779.
[19] C. D. Giovampaola, E. Martini, A. Toccafondi, and S. Maci, "Scatter-induced feed mismatch estimate by using a generalized spherical wave matrix approach," in *Proc. 5th Eur. Conf. Antennas Propag.*, Rome, Italy, Apr. 11–15, 2011, pp. 3939–3941.
[20] L. J. Chu, "Physical limitations of omni-directional antennas," *J. Appl. Phys.*, vol. 19, no. 12, pp. 1163–1175, 1948.
[21] S. J. Mason, "Feedback theory–Some properties of signal flow graphs," *Proc. IRE*, vol. 41, no. 9, pp. 1144–1156, Sep. 1953.
[22] D. M. Pozar, *Microwave Engineering*, 3rd ed. Hoboken, NJ: Wiley, 2005.
[23] W. Wasylkiwskyj and W. K. Kahn, "Theory of mutual coupling among minimum-scattering antennas," *IEEE Trans. Antennas Propag.*, vol. 18, no. 2, pp. 204–216, Mar. 1970.
[24] W. Wasylkiwskyj and W. K. Kahn, "Scattering properties and mutual coupling of antennas with prescribed radiation patterns," *IEEE Trans. Antennas Propag.*, vol. 18, no. 6, pp. 741–752, Nov. 1970.
[25] C.-T. Tai, *Dyadic Green's Functions in Electromagnetic Theory*. Scranton, PA: International Textbook, 1971.
[26] E. Martini, G. Carli, and S. Maci, "An equivalence theorem based on the use of electric currents radiating in free space," *IEEE Antennas Wireless Propag. Lett.*, vol. 7, pp. 421–424, 2008.
[27] M. Mohajer, S. Safavi-Naeini, and S. K. Chaudhuri, "Surface current source reconstruction for given radiated electromagnetic fields," *IEEE Trans. Antennas Propag.*, vol. 58, no. 2, pp. 432–439, Feb. 2010.
[28] D. M. Kerns, "Scattering-matrix description and nearfield measurements of electroacoustic transducers," *J. Acoustic Soc. Amer.*, vol. 57, no. 2, pp. 497–507, Feb. 1975.
[29] K. Atkinson, "Numerical integration on the sphere," *J. Australian Math. Soc. (Ser. B)*, vol. 23, pp. 332–347, 1982.
[30] T. Langer, A. Belyaev, and H.-P. Seidel, "Spherical barycentric coordinates," in *Proc. 4th Eurographics Symp. Geometry Process.*, Cagliari, Sardinia, Italy, 2006, pp. 81–88.
[31] R. S. Elliot, *Antenna Theory and Design*, Revised ed. Hoboken, NJ: Wiley-IEEE Press, 2003.
[32] F. Gronwald, S. Tkachenko, and J. Nitsch, "A comparison of different techniques for the calculation of antenna coupling within a cavity," presented at the Proc. XXVIII URSI Gen. Assembly, New Delhi, India, Oct. 23–29, 2005.
[33] F. Marliani and A. Ciccolella, "Computationally efficient expressions of the dyadic Green's function for rectangular cavities," *Progress Electromagn. Res.*, vol. 31, pp. 195–223, 2001.
[34] R. J. Pirkl, "Spatial autocovariances of S-parameter measurements in a lossy reverberation chamber," *IEEE Trans. Electromagn. Compat.*, submitted for publication.
[35] B. J. Cown and J. C. E. Ryan, "Near-field scattering measurements in determining complex target RCS," *IEEE Trans. Antennas Propag.*, vol. 37, no. 5, pp. 576–585, May 1989.
[36] B. Hauck, F. Ulaby, and R. DeRoo, "Polarimetric bistatic-measurement facility for point and distributed targets," *IEEE Antennas Propag. Mag.*, vol. 40, no. 1, pp. 31–41, Feb. 1998.
[37] K. Sarabandi and D. Zahn, "Bistatic scattering measurements using near-field scanning," in *IEEE 2001 Int. Geosc. Remote Sensing Symp.*, Sydney, Australia, Jul. 9–13, 2001, vol. 13, pp. 1359–1361.
[38] L. Gürel and H. Bağer, "Validation through comparison: Measurement and calculation of the bistatic radar cross section of a stealth target," *Radio Sci.*, vol. 38, no. 3, pp. 12:1–8, 2003.
[39] X. Zheng, "Statistics of impedance and scattering matrices in chaotic microwave cavities: The random coupling model," Ph.D. dissertation, Univ. Maryland, College Park, MD, 2005.
[40] S. D. Hemmady, "A wave-chaotic approach to predicting and measuring electromagnetic field quantities in complicated enclosures," Ph.D. dissertation, Univ. Maryland, College Park, MD, 2006.
[41] X. Zheng, T. M. A. Jr., and E. Ott, "Statistics of impedance and scattering matrices in chaotic microwave cavities: Single channel case," *Electromagnetics*, vol. 26, no. 1, pp. 3–35, Jan. 2006.
[42] X. Zheng, T. M. A. Jr., and E. Ott, "Statistics of impedance and scattering matrices of chaotic microwave cavities with multiple ports," *Electromagnetics*, vol. 26, no. 1, pp. 37–55, Jan. 2006.
[43] G. W. Stewart, *Matrix Algorithms: Basic Decompositions*. Philadelphia, PA: SIAM, 1998.
[44] R. B. Marks and D. F. Williams, "A general waveguide circuit theory," *J. Res. Nat. Inst. Standards Technol.*, vol. 97, no. 5, pp. 533–562, Sep. –Oct. 1992.

Ryan J. Pirkl (S'06–M'10) received the B.S., M.S., and Ph.D. degrees in electrical engineering from the Georgia Institute of Technology, Atlanta, in 2005, 2007, and 2010, respectively

For his graduate research, he developed hardware, measurement procedures, and processing tools for *in situ* characterization of radio wave propagation mechanisms. In 2010, he began working at the National Institute of Standards and Technology, Boulder, CO, under a National Research Council Postdoctoral Research Associateship. There, he investigated how reverberation chambers may be used as tunable wireless channel emulators for wireless device testing. In 2012, he joined the Subscriber Product Engineering Team, AT&T. His research interests include reverberation chambers, radio wave propagation, and analytical electromagnetics.